

A refined discrete triangular Mindlin element for laminated composite plates

Zengjie Ge[†] and Wanji Chen[‡]

Key Laboratories of the State for Structural Analysis of Industrial Equipment,
Dalian University of Technology, Dalian, P. R. China

(Received January 28, 2002, Accepted September 24, 2002)

Abstract. Based on the Mindlin plate theory, a refined discrete 15-DOF triangular laminated composite plate finite element RDTMLC with the re-constitution of the shear strain is proposed. For constituting the element displacement function, the exact displacement function of the Timoshenko's laminated composite beam as the displacement on the element boundary is used to derive the element displacements. The proposed element can be used for the analysis of both moderately thick and thin laminated composite plate, and the convergence for the very thin situation can be ensured theoretically. Numerical examples presented show that the present model indeed possesses the properties of higher accuracy for anisotropic laminated composite plates and is free of locking even for extremely thin laminated plates.

Key words: laminated composite plate; displacement function of Timoshenko's laminated beam; shear locking.

1. Introduction

The finite element method is ideally suited for the analysis of fiber-reinforced composites because it offers the versatility to model complicated geometries and loadings as well as varying material properties. There are three element models based on two-dimensional theories of laminated composite plates: 1) Kirchhoff model (Kirchhoff 1850), 2) Mindlin model (Mindlin 1951) and 3) high-order displacement model (Reddy 1984, Lo *et al.* 1977, Sheikh *et al.* 2002). In classical laminated theory (CLT) the usual Kirchhoff assumptions of plane sections remaining plane are effective, thereby neglecting shear deformations totally. When dealing with composite material applications, it is well known that this type of theory is too restrictive except in very thin plate applications. Thus, the theories used are that is attributed to the Mindlin type and high-order displacement type. The application of high-order displacement element is difficult because it has the complexity to derive the element formulations and the low efficiency of numerical evaluation. The Mindlin models based on first-order shear deformation theories (FSDT) are referred to as the constant shear angle theory (CST). In this case, a constant shear angle through the thickness of the plate is assumed. Actually, the shear deformation along the thickness of isotropic plate is quadratic.

[†] Ph.D.

[‡] Professor

For laminated composite plates the distribution of shear deformation is very complex. To reduce the error brought by this assumption (CST), some appropriate shear correction factor is chosen to account for the through-thickness shear deformation (Whitney 1973, Lardeur and Batoz 1989, Sze, He and Cheung 2000). To-date, FSDT is still considered the best compromise between the capability for prediction and computational cost for a wide class of applications. Some methods have been proposed to solve the above-mentioned problem of the FSDT. For example, the distribution of transverse shear stresses can be evaluated by three-dimensional (3D) elasticity equilibrium equation (Pryor *et al.* 1971). Vlachoutsis (1992) presented a simple procedure to calculate shear correction factors for laminated plates. Rolfes and Rohwer (1997, 1998) presented a simple post-processing approach to obtain improved transverse shear stresses in finite element analysis based on FSDT. New finite elements based on the FSDT are still proposed by many researchers (Singh *et al.* 1998, Sadek 1998, Auricchio and Sacco 1999, Kumar and Mukhopadhyay 2000). These efforts make it more convenient and reasonable to use the FSDT in practical applications.

During the past 30 years, many researchers have made significant contributions on the development of simple triangular and quadrilateral elements based on FSDT. The major problem is how to eliminate shear locking as the thickness-span ratio of the plate becomes small. It is well known that for Mindlin plates, only C^0 continuity is required and the difficulties of C^1 continuity requirement for thin plate elements can be avoided. Moreover, both the thin plate and the thick plate analysis can be integrated in the element model. Initial Mindlin plate elements used strain-displacement relations to obtain bending and transverse shear strain. In this case, bending energy is written in terms of nodal rotations only, whereas shear strain energy is given in terms of nodal rotation and deflections. When the plate becomes thin, transverse shear effects are reduced, and nodal deflections become associated only with vanishing shear energy. This is a difficult situation to uphold, and shear locking was soon observed. In order to avoid this, reduced integration (Zienkiewicz *et al.* 1971, Pugh *et al.* 1978) and selective integration technique (Malkus *et al.* 1978, Hughes *et al.* 1978) were widely used. For the 3-noded triangular element, a single Gauss point integration is used for calculating the shear strain energy. For the re-constituting shear strain technique, especially, the shear-strain approximation along the edge-projection or discrete Mindlin technique has been used to derive 3-noded triangular Mindlin plate elements. However, it is found that such elements have low accuracy, and furthermore they very often cannot pass the patch test for thin plates. It is fair to say, however, that the 9-DOF triangular Mindlin plate elements are less successful compared with either the quadrilateral or higher order triangular Mindlin plate elements. Therefore, there is a great interest in investigating new approaches, as the one discussed in this paper that can lead to formula 9-DOF triangular Mindlin plate elements with high performances.

Recently, a number of efficient 9-DOF triangular Mindlin plate elements based on the discrete constraint and the equilibrium conditions are produced (Batoz *et al.* 1989, 1992, Katili *et al.* 1993). These elements can converge towards the discrete Kirchhoff plate bending elements when the thickness of the plate is very thin. Furthermore, new quadrilateral Mindlin plate elements RDKTQM and triangular RDKTM with the re-constitution of the shear strain have been developed by Chen and Cheung (2000, 2001). Based on this method, the displacement function of the Timoshenko's beam is used in the formulation to derive new triangular thin/thick plate elements. The elements RDKQM and RDKTM indeed possess the properties of high accuracy for thin and thick plates, are capable of passing the patch test required for Kirchhoff thin plate elements, and do not exhibit extra zero energy modes. The elements RDKQM and RDKTM are free of locking for very thin plate

(where the thickness/span ratio is less than 10^{-30}) analysis and its convergence can be ensured theoretically.

In this paper, based on the triangular discrete Mindlin plate element RDKTM, a refined 15-DOF triangular discrete Mindlin element RDTMLC is formed by using the exact displacement function of the Timoshenko’s laminated composite beam as the displacement on the element boundary. The outline of this paper is as follows. In Section 2 and 3, the description of the element RDTMLC and the displacement function of the Timoshenko’s laminated composite beam are presented separately. In Section 4, formulations of membrane strain mode, bending strain mode and shear strain mode for element RDTMLC are derived. Numerical solutions of practical laminated composite plate problem are given in Section 5. Conclusions are drawn in Section 6.

2. Element description

The element RDTMLC is shown in Fig. 1. The displacement field is expressed as

$$\begin{aligned}
 U(x, y, z) &= u(x, y) + z\theta_x(x, y) \\
 V(x, y, z) &= v(x, y) + z\theta_y(x, y) \\
 W(x, y, z) &= w(x, y)
 \end{aligned}
 \tag{1}$$

in which x and y are the rectangular coordinates in the plane of the element, z is the thickness-direction coordinate measured upwards from the mid-plane; U , V , and W are the displacements in the x , y , and z directions respectively, u , v , and w are the corresponding mid-plane displacements, and θ_x and θ_y are the rotations.

Consider the Mindlin assumptions, the membrane, bending and transverse shear strains are related to the displacements and rotations by the following equations:

$$\begin{aligned}
 \boldsymbol{\varepsilon}_m &= [\partial u / \partial x \quad \partial v / \partial y \quad \partial u / \partial y + \partial v / \partial x]^T \\
 \boldsymbol{\varepsilon}_b &= [\partial \theta_x / \partial x \quad \partial \theta_y / \partial y \quad \partial \theta_x / \partial y + \partial \theta_y / \partial x]^T \\
 \boldsymbol{\varepsilon}_s &= [\theta_x - \partial w / \partial x \quad \theta_y - \partial w / \partial y]^T
 \end{aligned}
 \tag{2}$$

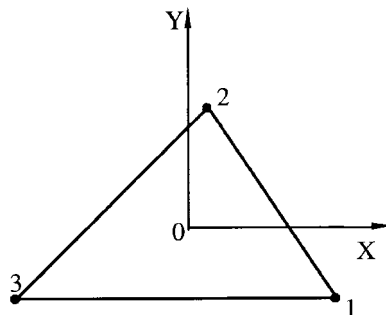


Fig. 1 The element RDTMLC in xy plane

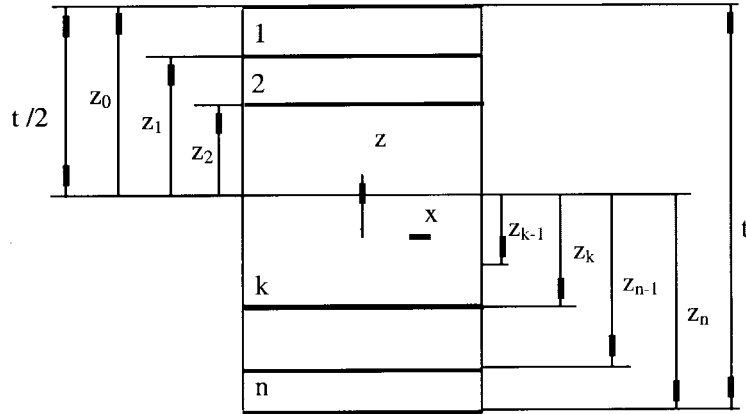


Fig. 2 The element RDTMLC in xz plane

The element strain energy can be written as

$$U^e = U_{mb} + U_s \tag{3}$$

where membrane-bending energy functional is given by

$$U_{mb} = \frac{1}{2} \int_{v_e} \begin{Bmatrix} \boldsymbol{\epsilon}_m \\ \boldsymbol{\epsilon}_b \end{Bmatrix}^T \begin{bmatrix} \mathbf{A} & \mathbf{B} \\ \mathbf{B} & \mathbf{D} \end{bmatrix} \begin{Bmatrix} \boldsymbol{\epsilon}_m \\ \boldsymbol{\epsilon}_b \end{Bmatrix} dv_e \tag{4}$$

and shear energy functional is given by

$$U_s = \frac{1}{2} \int_{v_e} \{\boldsymbol{\epsilon}_s\}^T [\mathbf{S}] \{\boldsymbol{\epsilon}_s\} dv_e \tag{5}$$

In Eqs. (4) and (5), \mathbf{A} , \mathbf{B} , \mathbf{D} and \mathbf{S} are extensional rigidity, flexural-extensional coupling rigidity, flexural rigidity and shear rigidity of laminated composite plate element, and v_e is the element domain.

For a laminated composite plate element (Fig. 2) consisting of n layers with element thickness t , the rigidity coefficients can be written as follows,

$$\begin{aligned} A_{ij} &= \sum_{k=1}^n (\bar{Q}_{ij})_k (z_k - z_{k-1}) \\ B_{ij} &= \frac{1}{2} \sum_{k=1}^n (\bar{Q}_{ij})_k (z_k^2 - z_{k-1}^2) \quad (i, j = 1, 2, 6) \\ D_{ij} &= \frac{1}{3} \sum_{k=1}^n (\bar{Q}_{ij})_k (z_k^3 - z_{k-1}^3) \\ S_{ij} &= \frac{5}{4} \sum_{k=1}^n (\chi_{ij} \bar{Q}_{ij})_k \left[z_k - z_{k-1} - \frac{4(z_k^3 - z_{k-1}^3)}{3t^2} \right] \quad (i, j = 4, 5) \end{aligned} \tag{6}$$

where $(\bar{Q}_{ij})_k$ are the elastic constants of layer k in the global coordinate direction of element, and it is necessary to transform from the principal laminate directions. $z_k(k = 0, 1, \dots, n)$ is the thickness-direction coordinate between layer k and layer $k + 1$. $(\chi_{ij})_k$ are the shear correction factors. For isotropic plates, $(\chi_{ij})_k = 5/6$. And for anisotropic plates, they must be calculated by using some special methods (Vlachoutsis 1992, Lardeur and Batoz 1989).

3. Timoshenko's laminated composite beam function

It is well known that when constructing a Mindlin plate element, both thick and thin plates should be taken into account, and it is necessary to eliminate the shear-locking phenomenon. To find such an element displacement function is definitely very difficult. Consider the refined element method, the interior strain or displacement of the element can be expressed in terms of the displacement on the boundary of the element. Note that a closed form solution for both thick and thin beams exists in the form of the Timoshenko's laminated beam function, and it is possible to use it to derive more efficient Mindlin laminated composite plate elements.

For a strip composite laminated plate with length L , width b , and thickness t , the governing equations can be written as follows,

$$\begin{aligned} \theta - \frac{dw}{dx} &= \frac{\bar{Q}_b d^2 \theta}{\bar{Q}_s dx^2} \\ \frac{d\theta}{dx} - \frac{d^2 w}{dx^2} &= \frac{q}{\bar{Q}_s} \end{aligned} \tag{7}$$

where \bar{Q}_b and \bar{Q}_s are bending elastic constant and shear elastic constant in the coordinate direction of element boundary (Fig. 3), and it is necessary to transform from the principal laminate directions. It should be noted that the well-known beam function is widely used in the approximation of various analytical functions. As the solution for slender beam, the beam function is expressed only in terms of the parameters of two endpoints of the beam without considering the distribution of load within the beam. Similarly, the Timoshenko's laminated beam function used in this paper is also based on this consideration. Neglecting the load q , (which will be taken care of in the consistent load matrix), we obtained

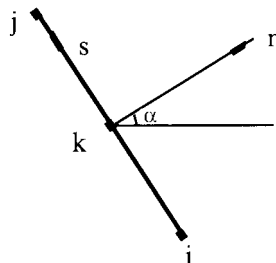


Fig. 3 Element boundary coordinate system

$$\theta - \frac{dw}{dx} = \lambda_e L^2 \frac{d^2\theta}{dx^2}$$

$$\frac{d\theta}{dx} - \frac{d^2w}{dx^2} = 0 \quad (8)$$

where $\lambda_e = \frac{\bar{Q}_b}{Q_s L^2}$.

The solutions satisfying the displacement w and the rotations θ at the two ends (node i and j) of the strip plate can be obtained as follows,

$$w = (L_i + \mu_e L_i L_j (L_i - L_j)) w_i + (L_i L_j + \mu_e L_i L_j (L_i - L_j)) L / 2 \theta_i$$

$$+ (L_j + \mu_e L_i L_j (L_j - L_i)) w_j + (-L_i L_j + \mu_e L_i L_j (L_i - L_j)) L / 2 \theta_j$$

$$\theta = -(6L_i L_j / L) \mu_e w_i + L_i (1 - 3\mu_e L_j) \theta_i$$

$$+ (6L_i L_j / L) \mu_e w_j + L_j (1 - 3\mu_e L_i) \theta_j \quad (9)$$

where $L_i = 1 - \frac{x}{L}$, $L_j = \frac{x}{L}$, $\mu_e = \frac{1}{1 + 12\lambda_e}$.

4. Finite element formulations

4.1 Displacement function of the element

In Fig. 4, the displacements of element are interpolated by six discrete nodes as follows,

$$\theta_x = \sum_{i=1}^6 N_i \theta_{xi}$$

$$\theta_y = \sum_{i=1}^6 N_i \theta_{yi}$$

$$w = \sum_{i=1}^6 N_i w_i \quad (10)$$

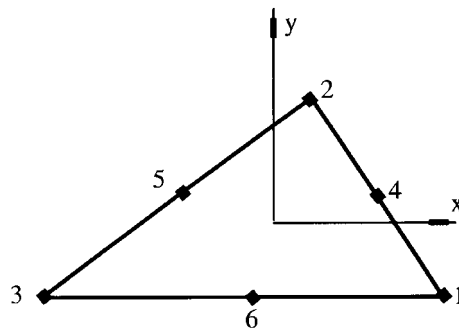


Fig. 4 6-nodes element with surplus mid-nodes

where N_i is the shape function of the 6-node triangular element in area coordinates (L_i), and

$$\begin{aligned} N_i &= (2L_i - 1)/L_i & (i = 1, 2, 3) \\ N_k &= 4L_iL_j & (k = 4, 5, 6; ij = 12, 23, 31) \end{aligned} \tag{11}$$

The surplus parameters θ_{xk} , θ_{yk} and w_k ($k = 4, 5, 6$) at the mid-node along the element boundary shown in Fig. 3 can be eliminated by the use of the interpolating function of the boundary displacement.

4.2 The explicit expression of the rotations θ_x and θ_y of the element

By using the parameters of the i and j nodes which are θ_{ni} , θ_{si} and θ_{nj} , θ_{sj} , the interpolation of the displacements $\tilde{\theta}_n$, $\tilde{\theta}_s$ on the $i - j$ boundary (see Fig. 3) can be given as

$$\tilde{\theta}_n = L_i\theta_{ni} + L_j\theta_{nj} \tag{12}$$

$$\begin{aligned} \tilde{\theta}_s &= -(6L_iL_j/S_{ij})\mu_{ij}w_i + L_i(1 - 3\mu_{ij}L_j)\theta_{si} \\ &+ (6L_iL_j/S_{ij})\mu_{ij}w_j + L_j(1 - 3\mu_{ij}L_i)\theta_{sj} \end{aligned} \tag{13}$$

where Eq. (13) is Timoshenko's beam function, $\mu_{ij} = 1/1 + 12\lambda_{ij}$, $\lambda_{ij} = \bar{Q}_b/\bar{Q}_s S_{ij}^2$, S_{ij} is the $i - j$ boundary length, and $\bar{L}_i = 1 - s/S_{ij}$ and $L_j = s/S_{ij}$ in which s is the coordinate along the boundary. The elastic constants \bar{Q}_b , \bar{Q}_s can be expressed as $\bar{Q}_b = D_{11}$, $\bar{Q}_s = S_{44}^*$ in which D_{11} and S_{44}^* can be obtained as D_{11} and S_{44} from Eq. (6), in which are replaced by the local coordinate directions along the boundaries of the element to the principle material directions. It is obvious that the displacement $\tilde{\theta}_s$ shown in Eq. (13) on the boundary will become the displacements of a thin plate boundary because $\lambda_{ij} \rightarrow 0$ when $t/S_{ij} \rightarrow 0$. (see Eq. (6), \bar{Q}_b/\bar{Q}_s is the function of t^2).

Substituting $L_i = L_j = 0.5$ into Eqs. (4) and (5), the θ_{nk} and θ_{sk} at the mid-side node k on the $i - j$ boundary can be obtained as follows,

$$\theta_{nk} = \frac{1}{2}(\theta_{ni} + \theta_{nj}) \tag{14}$$

$$\theta_{sk} = -\frac{1.5}{S_{ij}}\mu_{ij}w_i + \frac{1}{2}(1 - 1.5\mu_{ij})\theta_{si} + \frac{1.5}{S_{ij}}\mu_{ij}w_j + \frac{1}{2}(1 - 1.5\mu_{ij})\theta_{sj} \tag{15}$$

in which the θ_n and θ_s on the $i - j$ boundary shown in Fig. 1(b) can be expressed as

$$\begin{Bmatrix} \theta_n \\ \theta_s \end{Bmatrix} = \begin{bmatrix} l_{ij} & m_{ij} \\ -m_{ij} & l_{ij} \end{bmatrix} \begin{Bmatrix} \theta_x \\ \theta_y \end{Bmatrix} \tag{16}$$

where l_{ij} , m_{ij} are the direction cosines of the $i - j$ boundary.

Substituting Eq. (8) into Eqs. (6) and (7), we have for node k ,

$$\begin{Bmatrix} \theta_{xk} \\ \theta_{yk} \end{Bmatrix} = \mathbf{T}_k \begin{Bmatrix} w_i \\ \theta_{xi} \\ \theta_{yi} \\ w_j \\ \theta_{xj} \\ \theta_{yj} \end{Bmatrix} \tag{17}$$

where $\mathbf{T}_k = [\mathbf{T}_k^1 \ \mathbf{T}_k^2]$ and

$$\mathbf{T}_k^1 = \begin{bmatrix} 1.5m_{ij}\mu_{ij}/S_{ij} & -0.75\mu_{ij}m_{ij}^2 + 0.5 & 0.75\mu_{ij}l_{ij}m_{ij} \\ -1.5l_{ij}\mu_{ij}/S_{ij} & 0.75\mu_{ij}l_{ij}m_{ij} & -0.75\mu_{ij}l_{ij}^2 + 0.5 \end{bmatrix} \quad (18)$$

$$\mathbf{T}_k^2 = \begin{bmatrix} -1.5m_{ij}\mu_{ij}/S_{ij} & -0.75\mu_{ij}m_{ij}^2 + 0.5 & 0.75\mu_{ij}l_{ij}m_{ij} \\ 1.5l_{ij}\mu_{ij}/S_{ij} & 0.75\mu_{ij}l_{ij}m_{ij} & -0.75\mu_{ij}l_{ij}^2 + 0.5 \end{bmatrix} \quad (19)$$

$$\begin{Bmatrix} \theta_{xk} \\ \theta_{yk} \end{Bmatrix} = \mathbf{A}_k \mathbf{q}_b \quad (20)$$

where, $\mathbf{A}_k = [\mathbf{T}_k^1 \ \mathbf{T}_k^2 \ \mathbf{0}]$, $\mathbf{q}_b = [w_1 \ \theta_{x1} \ \theta_{y1} \ w_2 \ \theta_{x2} \ \theta_{y2} \ w_3 \ \theta_{x3} \ \theta_{y3}]^T$.

The explicit expression of the element rotations for describing bending strain of element can be obtained as follows,

$$\begin{Bmatrix} \theta_x \\ \theta_y \end{Bmatrix} = \sum_{i=1}^3 \left[N_i \begin{Bmatrix} \theta_{xi} \\ \theta_{yi} \end{Bmatrix} + N_{i+3} \mathbf{A}_{i+3} \mathbf{q}_b \right] = \tilde{\mathbf{N}} \mathbf{q}_b \quad (21)$$

where,

$$\tilde{\mathbf{N}} = [\tilde{\mathbf{N}}_1 \ \tilde{\mathbf{N}}_2 \ \tilde{\mathbf{N}}_3] \text{ and } \tilde{\mathbf{N}}_i = \begin{bmatrix} P_i & P_{xi} & P_{yi} \\ Q_i & Q_{xi} & Q_{yi} \end{bmatrix} \quad (i = 1, 2, 3). \quad (22)$$

For shape function $\tilde{\mathbf{N}}_1$,

$$\begin{aligned} P_1 &= 1.5_1(\mu_{12}m_{12}N_4/S_{12} - \mu_{31}m_{31}N_6/S_{31}) \\ P_{x1} &= -0.75(\mu_{12}m_{12}^2N_4 + \mu_{31}m_{31}^2N_6) + L_1 \\ P_{y1} &= 0.75(\mu_{12}l_{12}m_{12}N_4 + \mu_{31}l_{31}m_{31}N_6) \\ Q_1 &= 1.5(-\mu_{12}l_{12}N_4/S_{12} + \mu_{31}l_{31}N_6/S_{31}) \\ Q_{x1} &= 0.75(\mu_{12}l_{12}m_{12}N_4 + \mu_{31}l_{31}m_{31}N_6) \\ Q_{y1} &= -0.75(\mu_{12}l_{12}^2N_4 + \mu_{31}l_{31}^2N_6) + L_1 \end{aligned} \quad (23)$$

Other shape function $\tilde{\mathbf{N}}_i (i = 2, 3)$ can be obtained by cyclic permutation.

Finally, the rotation function of the refined element can be expressed as

$$\begin{Bmatrix} \theta_x \\ \theta_y \end{Bmatrix} = \tilde{\mathbf{N}} \mathbf{q}_b \quad (24)$$

where $\mathbf{q}_b = [w_1 \ \theta_{x1} \ \theta_{y1} \ w_2 \ \theta_{x2} \ \theta_{y2} \ w_3 \ \theta_{x3} \ \theta_{y3}]^T$.

4.3 The membrane-bending strain and the membrane-bending part of stiffness matrix of element

From standard elasticity theory the membrane-bending strain vector can be written as

$$\boldsymbol{\epsilon}_{mb} = \begin{bmatrix} 1 & z \\ 0 & 1 \end{bmatrix} \begin{Bmatrix} \boldsymbol{\epsilon}_m \\ \boldsymbol{\epsilon}_b \end{Bmatrix} \tag{25}$$

where $\boldsymbol{\epsilon}_m$ and $\boldsymbol{\epsilon}_b$ are given in Eq. (2).

The membrane displacement function of the element is given as (Fig. 1)

$$u = \sum_{i=1}^3 L_i u_i$$

$$v = \sum_{i=1}^3 L_i v_i \tag{26}$$

where $L_i (i = 1, 2, 3)$ are the area coordinates of the element, u_i, v_i are the nodal displacement parameters.

By using standard displacement finite element method, the membrane-bending strain vector can be expressed as

$$\boldsymbol{\epsilon}_{mb} = \mathbf{B}_{mb} \mathbf{q} \tag{27}$$

where \mathbf{B}_{mb} is the membrane-bending strain - displacement matrix of the element; \mathbf{q} is the displacement vector of the element, and it can be written as

$$\mathbf{q} = [u_1 \ v_1 \ w_1 \ \theta_{x1} \ \theta_{y1} \ u_2 \ v_2 \ w_2 \ \theta_{x2} \ \theta_{y2} \ u_3 \ v_3 \ w_3 \ \theta_{x3} \ \theta_{y3}]^T \tag{28}$$

The part of membrane-bending of the element stiffness matrix can be written as follows,

$$\mathbf{K}_{mb}^e = \int_{v_e} \mathbf{B}_{mb}^T \begin{bmatrix} \mathbf{A} & \mathbf{B} \\ \mathbf{B} & \mathbf{D} \end{bmatrix} \mathbf{B}_{mb} dv_e \tag{29}$$

4.4 The shear strain and the shear part of the stiffness matrix of element

The shear strain can be expressed as follows,

$$\boldsymbol{\epsilon}_s = \begin{Bmatrix} \gamma_x \\ \gamma_y \end{Bmatrix} = \begin{Bmatrix} \theta_x - \frac{\partial w}{\partial x} \\ \theta_y - \frac{\partial w}{\partial y} \end{Bmatrix} \tag{30}$$

$$\begin{Bmatrix} \gamma_x \\ \gamma_y \end{Bmatrix} = \begin{bmatrix} L_1 & 0 & L_2 & 0 & L_3 & 0 \\ 0 & L_1 & 0 & L_2 & 0 & L_3 \end{bmatrix} \begin{Bmatrix} \gamma_{x1} \\ \gamma_{y1} \\ \gamma_{x2} \\ \gamma_{y2} \\ \gamma_{x3} \\ \gamma_{y3} \end{Bmatrix} \quad (31)$$

In order to remove the shear locking, the Timoshenko's beam function can be used to define the rotation and deflection on the element boundary. The interpolation of the displacements \tilde{w}_s on the $i-j$ boundary (see Fig. 3) by using the parameters of the i and j nodes which are w_i , θ_{si} and w_j , θ_{sj} , can be given as

$$\begin{aligned} \tilde{w}_s &= (L_i + \mu_{ij}L_iL_j(L_i - L_j))w_i + (L_iL_j + \mu_{ij}L_iL_j(L_i - L_j))S_{ij}/2\theta_{si} \\ &\quad + (L_j + \mu_{ij}L_iL_j(L_j - L_i))w_j + (-L_iL_j + \mu_{ij}L_iL_j(L_i - L_j))S_{ij}/2\theta_{sj} \end{aligned} \quad (32)$$

and we have,

$$\begin{aligned} \frac{\partial \tilde{w}_s}{\partial s} &= \frac{1}{S_{ij}}(-1 + \mu_{ij}(1 - 6L_iL_j))w_i + 0.5(L_i - L_j + \mu_{ij}(1 - 6L_iL_j))\theta_{si} \\ &\quad + \frac{1}{S_{ij}}(1 - \mu_{ij}(1 - 6L_iL_j))w_j + 0.5(-L_i + L_j + \mu_{ij}(1 - 6L_iL_j))\theta_{sj} \end{aligned} \quad (33)$$

It is obvious that the displacements $\tilde{\theta}_s - \partial \tilde{w}_s / \partial s$ shown in Eqs. (13) and (33) on the boundary will always be constant because

$$\tilde{\theta}_s - \frac{\partial \tilde{w}_s}{\partial s} = (1 - \mu_{ij})w_i/S_{ij} + 0.5(1 - \mu_{ij})\theta_{si} - (1 - \mu_{ij})w_j/S_{ij} + 0.5(1 - \mu_{ij})\theta_{sj} \quad (34)$$

Therefore the shear strains at node i can be expressed by the constant shear strains. We have for node 1 (see Fig. 4),

$$\begin{Bmatrix} \gamma_{s4} \\ \gamma_{s6} \end{Bmatrix} = \begin{bmatrix} -m_{12} & l_{12} \\ -m_{31} & l_{31} \end{bmatrix} \begin{Bmatrix} \gamma_{x1} \\ \gamma_{y1} \end{Bmatrix} \quad (35)$$

and

$$\begin{Bmatrix} \gamma_{x1} \\ \gamma_{y1} \end{Bmatrix} = \frac{1}{l_{12}m_{31} - l_{31}m_{12}} \begin{bmatrix} l_{31} & -l_{12} \\ m_{31} & -m_{12} \end{bmatrix} \begin{Bmatrix} \gamma_{s4} \\ \gamma_{s6} \end{Bmatrix}. \quad (36)$$

Similarly, other nodal shear strains γ_{xi} and γ_{yi} ($i = 2, 3$) can be obtained by cyclic permutation.

Finally the shear strain can be obtained as follows,

$$\begin{aligned} \begin{Bmatrix} \gamma_x \\ \gamma_y \end{Bmatrix} &= \tilde{\mathbf{N}} \begin{Bmatrix} \gamma_{s4} \\ \gamma_{s5} \\ \gamma_{s6} \end{Bmatrix} \text{ and} \\ \tilde{\mathbf{N}} &= \begin{bmatrix} \bar{l}_3 L_1 - \tilde{l}_2 L_2 & \tilde{l}_1 L_2 - \hat{l}_3 L_3 & \hat{l}_2 L_3 - \bar{l}_1 L_1 \\ \bar{m}_3 L_1 - \tilde{m}_2 L_2 & \tilde{m}_1 L_2 - \hat{m}_3 L_3 & \hat{m}_2 L_3 - \bar{m}_1 L_1 \end{bmatrix} \end{aligned} \tag{37}$$

where

$$\bar{l}_i = \frac{l_i}{A_1}, \tilde{l}_i = \frac{l_i}{A_2}, \hat{l}_i = \frac{l_i}{A_3}, \bar{m}_i = \frac{m_i}{A_1}, \tilde{m}_i = \frac{m_i}{A_2}, \hat{m}_i = \frac{m_i}{A_3} \quad (i = 12, 23, 31),$$

$$A_1 = -l_{31}m_{12} + l_{12}m_{31}, \quad A_2 = -l_{12}m_{23} + l_{23}m_{12}, \quad A_3 = -l_{23}m_{31} + l_{31}m_{23},$$

$\gamma_{sk} (k = 4, 5, 6)$ are the natural shear strains at mid-side nodes 4, 5, 6 of the element (see Fig. 4), such that,

$$\begin{Bmatrix} \gamma_{s4} \\ \gamma_{s5} \\ \gamma_{s6} \end{Bmatrix} = \begin{Bmatrix} \theta_{s4} - \frac{\partial w_{s4}}{\partial s} \\ \theta_{s5} - \frac{\partial w_{s5}}{\partial s} \\ \theta_{s6} - \frac{\partial w_{s6}}{\partial s} \end{Bmatrix} \tag{38}$$

Substituting $L_i = L_j = 0.5$ into Eq. (35), we have for node k (see Fig. 3)

$$\theta_{sk} - \frac{\partial w_{sk}}{\partial s} = (1 - \mu_{ij})w_i/S_{ij} + 0.5(1 - \mu_{ij})\theta_{si} - (1 - \mu_{ij})w_j/S_{ij} + 0.5(1 - \mu_{ij})\theta_{sj} \tag{39}$$

It is obvious that $\gamma_x, \gamma_y \rightarrow 0$ when $(t/S_{ij})^2 \rightarrow 0, \mu_{ij} = 1$. The element RTDMLC is free of shear locking for thin plate analysis and its convergence can be ensured theoretically.

From Eq. (16) we have $\theta_s = [-m_{ij} \quad l_{ij}] \begin{Bmatrix} \theta_x \\ \theta_y \end{Bmatrix}$, then

$$\theta_{sk} - \frac{\partial w_{sk}}{\partial s} = \tilde{\mathbf{T}}_k \begin{Bmatrix} w_i \\ \theta_{xi} \\ \theta_{yi} \\ w_j \\ \theta_{xj} \\ \theta_{yj} \end{Bmatrix} \tag{40}$$

Finally, the mid-side node parameters $(\theta_{sk} - \partial w_{sk}/\partial s)$ of the element RTDMLC can be expressed as

$$\theta_{sk} - \frac{\partial w_{sk}}{\partial s} = \mathbf{B}_{sij} \mathbf{q} \quad (k = 4, 5, 6; \quad ij = 12, 23, 31) \tag{41}$$

The shear strain of the element RTDMLC can be obtained as follows:

$$\boldsymbol{\varepsilon}_s = \begin{Bmatrix} \theta_x - \frac{\partial w}{\partial x} \\ \theta_y - \frac{\partial w}{\partial y} \end{Bmatrix} = \tilde{\mathbf{N}} \begin{Bmatrix} \theta_{s4} - \frac{\partial w_{s4}}{\partial s} \\ \theta_{s5} - \frac{\partial w_{s5}}{\partial s} \\ \theta_{s6} - \frac{\partial w_{s6}}{\partial s} \end{Bmatrix} = \tilde{\mathbf{N}} \tilde{\mathbf{B}}_s \mathbf{q} = \mathbf{B}_s \mathbf{q} \quad (42)$$

where

$$\tilde{\mathbf{B}}_s = \begin{bmatrix} \mathbf{B}_{s12} \\ \mathbf{B}_{s23} \\ \mathbf{B}_{s31} \end{bmatrix} \quad (43)$$

The shear part of the stiffness matrix of the element RTDMLC can be written as follows,

$$\mathbf{K}_s^e = \int_{V_e} \mathbf{B}_s^T \mathbf{S} \mathbf{B}_s dv_e \quad (44)$$

Finally the stiffness matrix of element RTDMLC in the element local coordinate system can be written as follows,

$$\mathbf{K}^e = \mathbf{K}_{mb}^e + \mathbf{K}_s^e \quad (45)$$

Once the displacement variables are known the plane stresses $\boldsymbol{\sigma}_p$ are obtained by

$$\boldsymbol{\sigma}_p = z \mathbf{D}_{mb} \mathbf{B}_{mb} \mathbf{q} \quad (46)$$

and the transverse shear stresses given by Lardeur and Batoz (1989) can be obtained by integration of the 3D equilibrium equations using Eq. (46).

5. Numerical examples

In this section, a series of problems taken from various literature sources are used to determine the capability of the element to adequately predict the behavior of composite laminates. These problems involve varied boundary conditions, aspect ratios, loading conditions and laminate configurations. For several of these problems, comparisons are made with available 'exact' analytical solutions as well as other independent finite element solutions. The results are compared with finite element solutions of other models. These elements include a triangular element with high-order displacement model and several quadrangle elements. They are

MQH3T : hybrid element proposed by Spliker *et al.* (1985) which contains eight nodes with five DOF per node.

- SQUAD4 : mixed element proposed by Wilt *et al.* (1990) which contains four nodes with five DOF per node.
- TRIPLT : element proposed by Lakshminarayana and Murthy (1984), which contains three nodes with fifteen DOF per node.
- QUAD4 : four-node laminated anisotropic plate/shell element proposed by Somashekar *et al.* (1987).
- DST : discrete shear triangular element for composite plates proposed by Lardeur and Batoz (1989)

5.1 Two-layered angle-ply clamped square plates under uniform pressure

In this problem, a square two-layer plate ($a = 10, t = 0.02$, see Fig. 5) subjected to a uniformly distributed load $p = 100$ is considered. The clamped boundary conditions have all DOF restrained along the plate edge. The material properties for the problem are: $E_1 = 40 \times 10^6, E_2 = 1 \times 10^6, G_{12} = G_{23} = G_{31} = 0.5 \times 10^6, \nu_{12} = 0.25$.

The results of displacement \bar{w} at the center of the plate are given in Table 1. Note, \bar{w} is a nondimensional parameter, and it is given as $\bar{w} = (wE_2t^3/pa^4) \times 10^4$. The results are compared to exact solutions and other finite element solutions using the MQH3T element and the SQUAD4 element. MQH3T element used a 6×6 mesh (665 DOF), SQUAD4 element used a 10×10 mesh (605 DOF). The present 15-DOF triangular Mindlin plate element RDTMLC used 6×6 mesh (245 DOF), 8×8 mesh (405 DOF), and 10×10 mesh (605 DOF) for this case.

Again, due to the lackness of material symmetry, the entire plate was modeled.

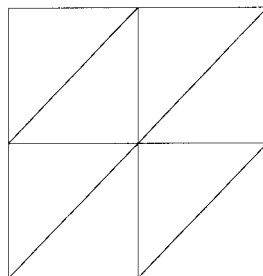


Fig. 5 Mesh (2 × 2) for quadrant of a square plate

Table 1 Normalized center deflection for clamped square plate with uniform pressure

Laminate	MQH3T	SQUAD4	R D T M L C			Exact
			6 × 6	8 × 8	10 × 10	
+5/-5	1.083	1.040	1.154	1.095	1.074	0.946
+15/-15	2.009	-----	1.919	1.944	1.959	1.691
+25/-25	2.572	2.602	2.378	2.466	2.508	2.355
+35/-35	2.844	2.914	2.611	2.726	2.782	2.763
+45/-45	2.929	3.013	2.687	2.809	2.868	2.890

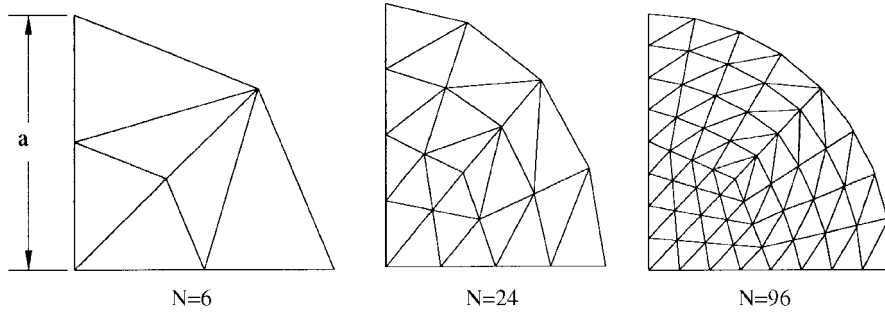


Fig. 6 Three meshes for quadrant of a circular plate

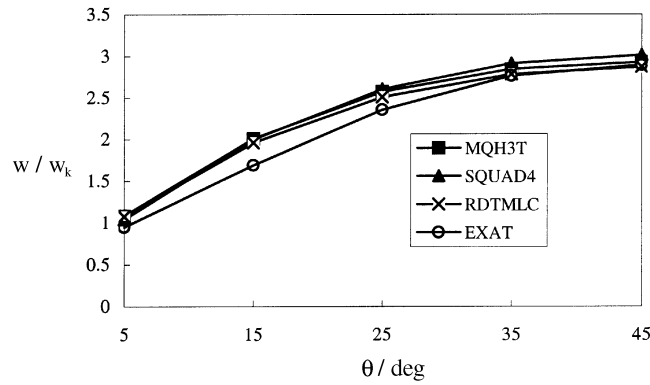


Fig. 7 The effect of fiber orientation θ on the convergence of the results

The effect of fiber orientation θ on the convergence of the results is shown in Fig. 7.

5.2 Two-layered angle-ply simply supported square plates under uniform pressure

The same plate as in Section 5.1 is considered. The plate is now simply supported on all four edges. The simply supported boundary conditions have, in addition to the transverse displacement, the in-plane displacement normal to the plate edge restrained. Table 2 shows some comparisons of plate center deflection w with the SQUAD4 element and the TRIPLT element used a 6×6 mesh (735 DOF). The SQUAD4 element that is the same as in Section 5.1 used a 10×10 mesh (605 DOF).

Table 2 Center deflections for simply supported square plate with uniform pressure

Laminate	TRIPLT	SQUAD4	R D T M L C			Exact
			6×6	8×8	10×10	
+5/-5	606	597	602	597	595	592
+15/-15	904	-----	863	877	883	893
+25/-25	992	1004	932	955	965	984
+35/-35	952	968	893	916	926	945
+45/-45	922	938	867	888	898	915

5.3 Cross-ply, laminated, square plate with clamped edges under a uniformly distributed load of intensity q

We consider a nine-layered, symmetrical laminate with [0/90/0/90/0/90/0/90/0] lay-up square plate. The total thickness of the 0° and 90° layers is the same. A high modulus graphite/epoxy composite material is used. The material properties for the problem are: $E_1 = 0.30 \times 10^8$, $E_2 = 0.75 \times 10^6$, $G_{12} = G_{31} = 0.45 \times 10^6$, $G_{23} = 0.375 \times 10^6$, $\nu_{12} = 0.25$. The plate is acted upon by a uniformly distributed load of intensity q , and has thickness t and side length a . The total thickness of all the 0° layers is the same as that of all 90° layers. Symmetry allows a quarter of the plate to be modeled. The correction factors are $\chi_{55} = 1.054$ and $\chi_{44} = 0.917$.

Table 3 shows the accuracy of the displacement at the center of plate w^* ($w^* = (wE_2t^3/qa^4) \times 10^3$) obtained by element RDTMLC with 6×6 , 8×8 and 10×10 meshes. In Table 3, the element TRIPLT results shown are based on a 4×4 mesh (375 DOF) of the quarter plate, the element QUAD4 based on an 8×8 mesh (405 DOF) of the quarter plate. The standard of comparison was taken to be the converged solution obtained by using the element SQH (Noor and Mathers 1975).

Table 3 Convergence of normalized center deflection for clamped nine-layered plate

t/a	TRIPLT	QUAD4	SQH	R D T M L C		
				6×6	8×8	10×10
0.1000	2.320	2.316	2.319	2.308	2.314	2.318
0.0100	0.964	0.957	0.963	0.982	0.973	0.969
0.0010	0.934	0.944	0.949	0.972	0.962	0.957
0.0001	-----	0.944	-----	0.972	0.962	0.957

5.4 Cross-ply, laminated, square plate with simply supported edges under a uniformly distributed load of intensity q

We consider the same plate as in Section 5.3. The plate is now simply supported on all four edges. Table 4 shows some comparisons with the exact solutions and other finite element solutions using the TRIPLT and QUAD4. The TRIPLT and the QUAD4 are same as in Section 5.3.

The effect of decreasing thickness ratio t/a on the convergence of the results is shown in Fig. 8.

Table 4 Convergence of normalized center deflection for cross-ply, nine-layered plate with simply supported edges under a uniformly distributed load

t/a	TRIPLT	QUAD4	R D T M L C			Exact
			6×6	8×8	10×10	
0.1000	5.85	5.84	5.859	5.858	5.858	5.85
0.0100	4.48	4.47	4.479	4.482	4.483	4.49
0.0010	4.45	4.46	4.468	4.470	4.471	4.47
0.0001	-----	4.46	4.468	4.470	4.470	-----

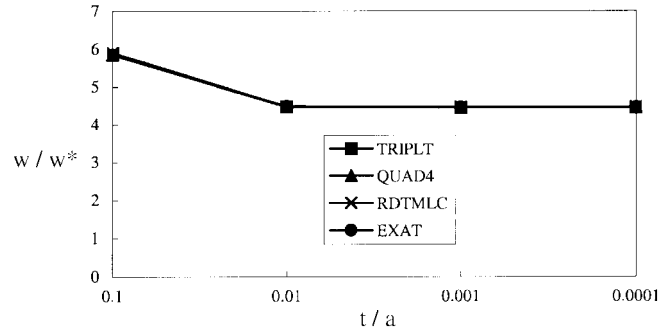


Fig. 8 The effect of decreasing thickness ratio t/a on the convergence of the results

5.5 Cross-ply, laminated, square plate with simply supported edges under a doubly sinusoidal loading

This example, proposed by Pagano and Hatfield (1972), is the same plate as in Section 5.4. The plate is acted upon by a doubly sinusoidal distributed load of intensity $q = q_0 \sin \frac{\pi x}{a} \sin \frac{\pi y}{a}$. The

material properties for the problem are: $E_1 = 25 \times 10^6$, $E_2 = 1 \times 10^6$, $G_{12} = G_{31} = 0.5 \times 10^6$, $G_{23} = 0.2 \times 10^6$, $\nu_{12} = 0.25$. The total thickness of all the 0° layers is the same as that of all 90° layers. The correction factors are given by Lardeur and Batoz (1989) which are $\chi_{55} = 0.689$ and $\chi_{44} = 0.611$. Three different meshes, i.e., (6×6) , (8×8) and (10×10) , are used to model a quadrant of the plate, and five a/t aspect ratios are considered.

Displacement and stress are given in the form

$$\tilde{w} = w \pi^4 Q / 12 S^4 t q_0 \text{ with } S = a/t \text{ and } Q = 4G_{12} + (E_1 + E_2(1 + 2\mu_{23})) / (1 - \mu_{12}\mu_{21})$$

(Note: $\mu_{23} = 0.25$ here. It is necessary for 3 D elastic solution, but it is no need for FDST); $(\tilde{\sigma}_x, \tilde{\sigma}_y, \tilde{\tau}_{xy}) = 1/q_0 S^2 (\sigma_x, \sigma_y, \tau_{xy})$. The results obtained together with some other solutions are presented in Table 5. It is noted that the transverse shear stresses are obtained by integration of the 3D equilibrium equations and these are not listed in Table 5.

5.6 A clamped circular plate with uniform pressure

A circular plate of radius a with clamped edge under uniformly distributed load of intensity q is considered. The material is a unidirectional laminate, with the material fibers at an angle $\theta = 0$ with respect to the global coordinate. Due to symmetry only one-quarter of the plate was modeled using mesh sizes of 6, 24, and 96 elements (see Fig. 6). In this problem, the material properties are: $E_1 = 5.6 \times 10^6$, $E_2 = 1.2 \times 10^6$, $G_{12} = G_{23} = G_{31} = 0.6 \times 10^6$, $\nu_{12} = 0.26$. Table 6 gives comparison of center deflection of circular plate with the exact solutions and QUAD4 element. The QUAD4 element is same as in Section 5.4, and its results shown are based on mesh sizes of 3, 12, and 48 elements for one-quarter of the plate. Note that the quantities in the Table 6 are normalized deflections, w^* , i.e., $w^* = wD/qa^4$, where $D = 3(D_{11} + D_{22}) + 2(D_{12} + 2D_{66})$ and D_{11} , D_{22} , D_{12} , and D_{66} are bending rigidity coefficients found by laminate theory.

Table 5 Maximum deflection and stresses for cross-ply, nine-layered plate with simply supported edges under a doubly sinusoidal distributed load

a/t	Model	Mesh	$\tilde{w}\left(\frac{a}{2}, \frac{a}{2}, 0\right)$	$\tilde{\sigma}_x\left(\frac{a}{2}, \frac{a}{2}, \pm\frac{t}{2}\right)$	$\tilde{\sigma}_y\left(\frac{a}{2}, \frac{a}{2}, \pm\frac{2t}{5}\right)$	$\tilde{\tau}_{xy}\left(0, 0, \pm\frac{t}{2}\right)$
4	RD TLC M	6 × 6	4.227	± 0.469	± 0.541	∓ 0.0219
		8 × 8	4.217	± 0.461	± 0.539	∓ 0.0220
		10 × 10	4.212	± 0.457	± 0.538	∓ 0.0220
	DST	10 × 10	4.242	± 0.547	± 0.419	-----
	3D elasticity		4.079	± 0.720	± 0.663	-----
	FSDT		4.242	± 0.491	± 0.487	∓ 0.0217
10	RD TLC M	6 × 6	1.522	± 0.517	± 0.481	∓ 0.0216
		8 × 8	1.524	± 0.510	± 0.478	∓ 0.0216
		10 × 10	1.524	± 0.507	± 0.477	∓ 0.0216
	DST	10 × 10	1.526	± 0.541	± 0.425	-----
	3D elasticity		1.512	± 0.551	± 0.477	∓ 0.0233
	FSDT		1.522	± 0.519	± 0.454	∓ 0.0215
50	RD TLC M	6 × 6	1.015	± 0.545	± 0.435	∓ 0.0213
		8 × 8	1.017	± 0.543	± 0.435	∓ 0.0213
		10 × 10	1.019	± 0.541	± 0.434	∓ 0.0213
	DST	10 × 10	1.020	± 0.522	± 0.447	-----
	3D elasticity		1.021	± 0.539	± 0.433	∓ 0.0214
	FSDT		1.021	± 0.538	± 0.432	∓ 0.0213
100	RD TLC M	6 × 6	1.000	± 0.545	± 0.433	∓ 0.0213
		8 × 8	1.002	± 0.543	± 0.433	∓ 0.0213
		10 × 10	1.003	± 0.541	± 0.432	∓ 0.0213
	3D elasticity		1.005	± 0.539	± 0.431	∓ 0.0213
	FSDT		1.005	± 0.538	± 0.431	∓ 0.0213
	100,000	RD TLC M	6 × 6	0.995	± 0.544	± 0.433
8 × 8			0.997	± 0.542	± 0.432	∓ 0.0213
10 × 10			0.998	± 0.541	± 0.431	∓ 0.0213
3D elasticity			1.000	± 0.539	± 0.431	∓ 0.0213
FSDT			1.000	± 0.539	± 0.431	∓ 0.0213

Table 6 Normalized center deflection of circular plate

a/t	S Q U A D 4			R D T M L C			Exact
	3	12	48	6	24	96	
1000	0.1163	0.1231	0.1246	0.1360	0.1310	0.1265	0.1250
100	0.1193	0.1242	0.1249	0.1361	0.1311	0.1266	-----
50	0.1211	0.1247	0.1253	0.1362	0.1313	0.1268	-----
25	0.1237	0.1264	0.1270	0.1366	0.1319	0.1276	-----
16.67	0.1266	0.1291	0.1297	0.1375	0.1331	0.1291	-----
10	0.1355	0.1378	0.1384	0.1408	0.1376	0.1344	-----

Variation of normalizing center deflection of circular plate with decreasing thickness ratio t/a is shown in Fig. 9.

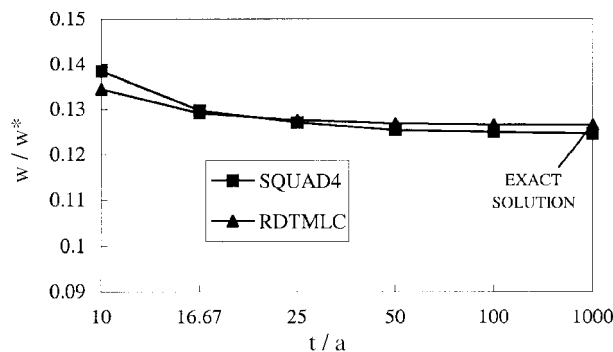


Fig. 9 Variation of normalizing center deflection of circular plate with decreasing thickness ratio $(\bar{Q}_{ij})_k$

6. Conclusions

Based on the preceding discussions and the numerical examples, the following conclusions can be drawn.

- (1) The exact solution of the Timoshenko's laminated beam as a displacement of the boundary of the element can be used to derive the Mindlin laminated composite plate element. This results in the thin and thick laminated composite plate analysis being integrated in a uniform model and the convergence for very thin laminated composite plate can be ensured theoretically.
- (2) The proposed triangular discrete Mindlin laminated composite plate element RDTMLC is a re-constitution shear strain element. The element RDTMLC based on first-order shear deformation theories, and it possesses higher accuracy when the span/thickness ratios more than 10. It is also free from shear locking for extremely thin laminate plates.
- (3) Based on the results from numerical evaluation, the proposed element has satisfactory rate of convergence and acceptable accuracy within reasonable mesh refinement for multilayer laminated plates of both homogeneous isotropic and laminated anisotropic materials. The formulations of the element RDTMLC are simpler, so it can be considered as the most efficient and simplest one among the 15-DOF triangular laminated composite plate elements.

References

- Auricchio, F. and Sacco, E. (1999), "A mixed-enhanced finite-element for the analysis of laminated composite plates", *Int. J. Num. Meth. Eng.*, **44**, 1481-1504.
- Auricchio, F. and Sacco, E. (1999), "Partial-mixed formulation and refined models for the analysis of composite laminates within an FSDT", *Composite Structures*, **46**, 103-113.
- Batoz, J.L. and Lardeur, P. (1989), "A discrete shear triangular nine d.o.f. element for the analysis of thick to very thin plates", *Int. J. Num. Meth. Eng.*, **29**, 533-560.
- Batoz, J.L. and Katili, I. (1992), "On a simple triangular Reissner/Mindlin plate element based on incompatible modes and discrete constraints", *Int. J. Num. Meth. Eng.*, **35**, 1603-1632.
- Chen, Wanji and Cheung, Y.K. (2000), "Refined quadrilateral element based on Mindlin/Reissner plate theory", *Int. J. Num. Meth. Eng.*, **47**, 605-627.
- Chen, Wanji and Cheung, Y.K. (2001), "Refined 9-DOF triangular Mindlin plate element", *Int. J. Num. Meth. Eng.*, **51**, 1259-1281.

- Hughes, T.J.R., Cohen, M. and Haroun, M. (1978), "Reduced and selective integration techniques in finite element analysis of plates", *Nucl. Eng. Design*, **46**, 203-222.
- Katili, I. (1993), "A new discrete Kirchhoff-Mindlin element based on Mindlin-Reissner plate theory and assumed shear strain fields-Part I: An extended DKT element for thick-plate bending analysis", *Int. J. Num. Meth. Eng.*, **36**, 1859-1883.
- Kirchhoff, G. (1850), "Über das gleichgewicht und bewegung einer elastischen schein", *Journal für die reine und angewandte Math.*, **40**, 51-88.
- Lakshminarayana, H.V. and Murthy, S.S. (1984), "A shear-flexible triangular finite element model for laminated composite plates", *Int. J. Num. Meth. Eng.*, **20**, 591-623.
- Lardeur, P. and Batoz, J.L. (1989), "Composite plane analysis using a new discrete shear triangular finite element", *Int. J. Num. Meth. Eng.*, **27**, 343-359.
- Lo, K.H., Christensen, R.M. and Wu, E.M. (1977), "A higher-order theory of plate deformation. Part 2: laminated plates", *J. Appl. Mech.*, **44**, 669-676.
- Malkus, D.S. and Hughes, T.J.R. (1978), "Mixed finite element methods-reduced and selective integration techniques: a unification of concepts", *Comput. Meth. Appl. Mech. Eng.*, **15**, 63-81.
- Mindlin, R.D. (1951), "Influence of rotary inertia and shear on flexural motions of isotropic elastic plates", *J. Appl. Mech.*, **18**, 31-38.
- Noor, A.K. and Mathers, M.D. (1975), "Shear-flexible finite element method of laminated composite plates", *NASA TN D-8044*.
- Pagano, N.J. and Hatfield, S.J. (1972), "Elastic behavior of multilayered bi-directional composites", *AIAA J.*, **10**, 931-933.
- Pryor, C.W. and Barker, R.M. (1971), "A finite element analysis including transverse shear effects for application to laminated plates", *AIAA J.*, **9**, 912-917.
- Pugh, E.D., Hinton, E. and Zienkiewicz, O.C. (1978), "A study of triangular plate bending element with reduced integration", *Int. J. Num. Meth. Eng.*, **12**, 1059-1078.
- Reddy, J.N. (1984), "A simple higher-order theory for laminated composite plates", *J. Appl. Mech.*, **51**, 745-752.
- Rolfes, R. and Rohwer, K. (1997), "Improved transverse shear stresses in composite finite elements based on first order shear deformation theory", *Int. J. Num. Meth. Eng.*, **40**, 51-60.
- Rolfes, R., Rohwer, K. and Ballerstaedt, M. (1998), "Efficient linear transverse normal stress analysis of layered composite plates", *Comput. Struct.*, **68**, 643-652.
- Sadek, E.A. (1998), "Some serendipity finite element for the analysis of laminate plates", *Comput. Struct.*, **69**, 37-51.
- Satish Kumar, Y.V. and Madhujit Mukhopadhyay (2000), "A new triangular stiffened plate element for laminate analysis", *Composites Science and Technology*, **60**, 935-943.
- Sheikh, A.H., Haldar, S. and Sengupta, D. (2002), "A high precision shear deformable element for the analysis of laminated composite plates of different shapes", *Comput. Struct.*, **55**, 329-336.
- Singh, G., Raju, K.K. and Rao, G.V. (1998), "A new lock-free, material finite element for flexure of moderately thick rectangular composite plates", *Comput. Struct.*, **69**, 609-623.
- Somashekar, B.R., Prathap, G. and Ramesh, B.C. (1987), "A field consistent four-node laminated anisotropic plate/shell element", *Comput. Struct.*, **25**(3), 345-353.
- Spilker, R.L., Jakobs, D.M. and Engelmann, B.E. (1985), "Efficient hybrid stress isoparametric elements for moderately thick and thin multi-layer plates", In: Spilker, R.L. and Reed, K.W., editors. *Hybrid and Mixed Finite Element Methods*, ASME, AMD-vol-73, New York.
- Sze, K.Y., He, L.W. and Cheung, Y.K. (2000), "Predictor-corrector procedures for analysis of laminated plates using standard Mindlin finite element models", *Composite Structures*, **50**, 171-182.
- Whitney, J.M. (1973), "Shear correction factors for orthotropic laminates under static load", *J. Appl. Mech.*, **40**, 302-304.
- Wilt, T.E., Saleeb, A.F. and Chang, T.Y. (1990), "A mixed element for laminated plates and shells", *Comput. Struct.*, **37**(4), 597-611.
- Vlachoutsis, S. (1992), "Shear correction factors for plates and shells", *Int. J. Num. Meth. Eng.*, **33**, 1537-1552.
- Zienkiewicz, O.C., Taylor, R.L. and Too, J.M. (1971), "Reduced integration technique in general analysis of plates and shells", *Int. J. Num. Meth. Eng.*, **3**, 275-290.